eJSE INTERNATIONAL

Investigating the Behaviour and Strength of Unbonded Pre-tensioned RC Slabs Subject to Flexural Loads

Jasmin Abdelhalim[a], George Iskander[b], Ezzeldin Sayed-Ahmed[a]
[a] The American University in Cairo (AUC), Egypt
[b] University of Calgary, Canada
*Corresponding author: jasminosama@aucegypt.edu

Abstract

Unbonded pre-tensioned systems, in which tendons are greased and wrapped in plastic sheathing, have several benefits in comparison to bonded systems. However, analytical evaluation of their capacity is taxing due to the iterative compatibility conditions necessary to determine the system's behavior using the empirical equations available in the literature. To investigate the behaviour and strength of unbonded pre-tensioned RC slabs subject to flexural loads, four simply supported post-tensioned slabs with unbonded tendons were tested in flexure. Experimental failure loads and tendon strains were compared to the ACI 318-19 provisions. While the provisions for unbonded specimens were found to be accurate, the strain in the unbonded tendons exceeded the yield stress in all specimens, suggesting that ACI 318-19's stress limitations on unbonded post-tensioned concrete are unwarranted. The unbonded system also showed better crack control at the failure stage when non-prestressing steel reinforcement is used when compared to system with no non-prestressing steel.

1. Introduction

Prestressed concrete has become ubiquitous in the construction sector for its desirable tensile, durability, and sustainability characteristics. Prestressed concrete is characterized by an improved tensile strength (Süleymanoğlu et al. 2017), offering more flexibility in concrete structural design. The option of greasing and sheathing prestressing tendons improves reinforcement durability in severe environments, increasing structural durability (Süleymanoğlu et al. 2017). From a sustainability perspective, prestressed concrete's improved tensile strength permits the use of slenderer cross-sections, reducing material intensity and thereby lowering the embodied energy of a given structure.

The tendons in a prestressed concrete specimen may be tensioned prior to concrete casting (pre-tensioning) or tensioned after the concrete achieves certain strength (post-tensioning) (Bondy et al. 2006). This paper will only consider post-tensioned specimens.

1.1 Post-tensioning techniques

Broadly speaking, post-tensioning techniques fall into two categories: bonded or unbonded. The difference between these techniques, as the names suggest, is the existence of bond between the surrounding concrete and the prestressing tendons (Ellobody et al. 2008). In unbonded systems, prestressing tendons are covered with grease and wrapped with plastic sheathing, as shown in Figure 1a. The grease and plastic prevent the formation of bond with the surrounding concrete; instead, the tendon force is transferred to the concrete through the anchors. A clear advantage of this system is that the plastic and grease provide the tendons protection against moisture and chemicals, as well as damage from mechanical handling. However, unbonded systems have several shortcomings such as the associated complicated analysis and the non-uniform strain along the tendons due to the transferring mechanism at the anchor locations (Hussien, 2012 and Oukaili, 2022). Moreover, the strain of unbonded tendons depends on the interaction between the anchorage and the concrete. If the concrete in the compression zone around the anchors experiences any creep, shrinkage or elastic deformation, the strain of the unbonded tendons changes accordingly (Oukaili, 2022). In bonded systems, ducts are cast-in the specimen; tendons are inserted in these ducts and tensioned, then they are filled with grout to ensure compatibility with the surrounding material (Aalami, 1994), as shown in Figure 1b.

In addition to the durability benefits of unbonded construction conferred by the plastic and grease layers, there are several advantages associated with unbonded post-tensioning. Unbonded construction is easier and faster to install, owing to the higher flexibility and maneuverability of the sheathed tendons compared to duct installation. Unbonded construction speed is also increased in relation to bonded

construction as one does not need to wait for grout to cure. Unbonded construction also provides ease of repair and replacement, as damaged tendons can simply be pulled out and replaced – in contrast, bonded tendons are almost impossible to remove from a member. Further, ducts are prone to several problems such as blockage, collapse, or shifting due to temperature fluctuations (Aalami, 1994).
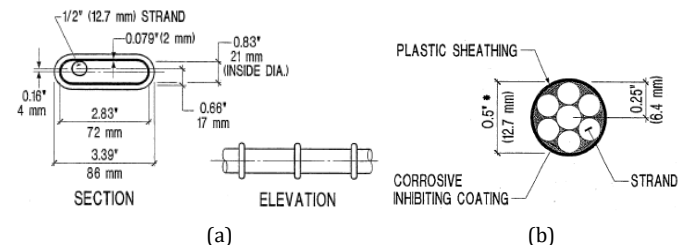
Fig. 1 (a) 7-Wire Unbonded Tendon (12.7mm) (Aalami, 1994)

(b) Plastic Flat Corrugated Duct (Aalami, 1994)

1.2 Factors influencing post-tensioned flexural behaviour

Significant research has been conducted to investigate the difference in behavior between unbonded and bonded prestressed flexural specimens. Mattock et al. (1971) constructed and tested seven simply supported and three continuous beams in accordance with ACI-318-19 provisions and found that simply supported bonded beams had up to a 20% higher ultimate moment than the unbonded beams. The authors attributed this difference to the additional area of steel provided by the steel ducts for the bonded specimens. In contrast, cook et al. (1981) tested 9 simply supported slabs of unbonded tendons and 3 simply supported slabs of bonded tendons identical in all aspects to the unbonded slabs. There was no additional crack control reinforcement to the unbonded specimens; the authors found similar ultimate moment resistances in both cases. Naaman et al. (1991) showed that ACI 318-83's equations were conservative because it estimated the ultimate stress of unbonded tendons to range between the effective prestress value and the yield stress of the cable.

Modern studies also show that this approach is conservative. Ellobody et al. (2008) used a nonlinear finite element model verified against the test results of two slabs to conduct a parametric study of post-tensioned unbonded one-way slabs in bending. The authors examined the influence of slab depth, tendon forces, boundary conditions and concrete strength. The models showed that the ACI 318-19's stress limitations on unbonded prestressed sections are conservative. Additionally, Yang et al. (2013) used the test data of 188 beams and lightweight concrete post-tensioned

slabs to propose a new equation for the unbounded tendon's ultimate stress; the authors found excellent agreement with the data when taking the ultimate stress in the tendons to exceed the yield point.

Ellobody, et al. (2008) used the results of their parametric study to compare the British Standards (BS8110-01, 1997) unbonded tendon's ultimate stress equation and their verified non-linear finite element model. The results of the FE model showed higher values for the ultimate loads than the results of the code equations. The authors concluded from this study that the reason behind the code equation conservation is the limitation of the unbonded tendon's ultimate stress.

Mojtahedi and Gamble (1978) investigated the influence of span-to-depth ratio on the flexural behaviour of unbonded specimens. The authors tested simple beams, continuous beams, and continuous slabs with unbonded tendons and varying span-to-depth ratio and concluded that increased span-to-depth ratios significantly reduce the unbonded tendon's ultimate stress value. Mojtahedi and Gamble additionally developed a truss model for an unbonded cracked prestressed beam which supported their experimental findings.

1.3 ACI 318-19 provisions

ACI 318-19 computes unbonded tendon ultimate stress as being in the range of the effective prestressing stress and the yield stress in the interest of conservatism. Further, ACI 318-19 agrees with the findings of Mojtahedi and Gamble (1978) and varies the stresses computed in unbonded tendons with the span-to-depth ratio. These limitations are not imposed on bonded systems.

For prestressed sections with unbonded prestressing and span-to-depth ratios less than or equal to 35, the nominal flexural strength (f_{ps}) of the unbonded tendon is the least of the empirical Equations 1, 2, and 3, according to ACI 318-19, section 20.3.2.4.1, where f_{pe} is the effective prestressing stress in the tendons, f_{py} is the prestressing tendon yield stress, $f_c^/$ is the surrounding concrete's cylinder strength, and σ_{ps} is the prestressing steel reinforcement ratio.

$$f_{ps} = f_{pe} + 70 + \frac{f_c^/}{100\rho_{ps}} \qquad (1)$$
$$f_{ps} = f_{pe} + 420 \qquad (2)$$
$$f_{ps} = f_{py} \qquad (3)$$

For unbonded prestressed members with span-to-depth ratio exceeding 35, the nominal flexural strength (f_{ps}) of the unbonded tendon is the least of the three equations 3, 4, and 5.

$$f_{ps} = f_{pe} + 70 + \frac{f_c^/}{300\rho_{ps}} \qquad (4)$$
$$f_{ps} = f_{pe} + 210 \qquad (5)$$

For prestressed members with bonded tendons the ACI 318-19 provisions allow strain compatibility analysis to calculate the nominal flexural strength (f_{ps}). Another difference of significance is that minimum crack control reinforcement is additionally required by ACI 318-19 in unbonded prestressed one-way slabs, but not for bonded slabs.

According to the ACI 318-19 provisions the bonded tendon's nominal strength is higher than the nominal strength allowed for the unbonded tendons. ACI 318-19 also states that crack control non-prestressed steel reinforcement must be used in case of unbonded tendons.

2. Research Significance

ACI 318-11 underestimates the strength of unbonded pretensioned flexural members by limiting unbonded tendon's ultimate stress to the tendon's yield stress (Yang et al. (2013) and He and Liu (2010)). This research aims to investigate the accuracy of the ACI 318-19 provisions on Unbonded Flexural Design. To investigate the suitability of ACI 318-19 design provisions for unbonded systems, four simply supported post-tensioned slabs with unbonded tendons were tested in flexure. Experimental failure loads and tendon strains were compared to the ACI 318-19 provisions. The ACI 318-19's predicted nominal strengths were accurate. However, the tendons in all cases yielded in contrary with the ACI 318-19's prediction.

3. Experimental Program

An experimental program was conducted to investigate the adequacy of ACI 318-19 design provisions for unbonded post-tensioned slabs and the necessity of adding crack control reinforcement to such members. This study contributes valuable experimental data on post-tensioned slab specimens in addition to examining the requirement for shrinkage reinforcement in unbonded systems. Post-tensioned slabs with unbonded tendons were loaded to failure to investigate tendon stresses at ultimate conditions; obtained ultimate tendon stresses were compared with ACI 318-19 design provisions.

Two sets of duplicate post-tensioned slab specimens were constructed. All slabs were 4.0 m in span, 1.0 m in width, and 0.16 m in depth, and contained three prestressing tendons. The geometry of the specimens was chosen to represent commonly found slabs that fail in flexural without additional shear reinforcement. The first set of duplicates was only reinforced with unbonded post-tensioned tendons (specimens UBS1 and UBS2) while the second set of duplicates was reinforced with unbonded post-tensioned tendons and 10M bars spaced at 200 mm crack control reinforcement as per ACI 318-19 provisions (specimens UBSR1 and UBSR2). All specimens were subjected to a four-point bending test. Failure load, strain and behaviour of specimens were recorded throughout the test.

3.1 Specimen design

Normal weight concrete with a 7 and 28-day cube strength of 26.4 and 40 MPa, respectively, was used to cast all specimens. Prestressing normal relaxation 7-wire strands tendons were supplied by STRANDS Company - Egypt ("STRANDS"). The tendons were 12.7 mm in diameter with yield and ultimate stresses of 1674 MPa and 1860 MPa, respectively. GTI Company - USA supplied the encapsulated zero void anchorage system used for the unbonded slabs. Figure 2a shows the traditional anchor used for the bonded system supplied by STRANDS, while Figure 2b shows the encapsulated zero-void anchor provided by GTI.

(a)   (b)

Fig. 2 (a) Anchor for the bonded system, provided by Strands Company, Egypt. (b) Encapsulated Anchor for the Unbonded System, provided by GTI, USA.

The tendon profile used in all slabs was a double-harped shape, with a maximum eccentricity at mid span of 0.04 m and zero eccentricity at the slab edges. The tendon eccentricity varied linearly from 0 at the ends to 0.04 m at 1.5 from the slab ends. The eccentricity was kept constant (0.04 m) at the middle 1.3 m. Tendons were spaced at 0.333 m and an edge distance was 0.167 m. The tendon profile is shown in Figures 3 and 4.

For all slabs, spiral stirrups and closed rectangular stirrups are added to resist the stresses generated in local and general anchorage zones, as shown in Figures 3 and 4. In addition, rectangular closed stirrups (10M @ 200 mm) were distributed over the first meter of the span in the longitudinal and transverse directions for all specimens, as shown in Figures 3 and 4.
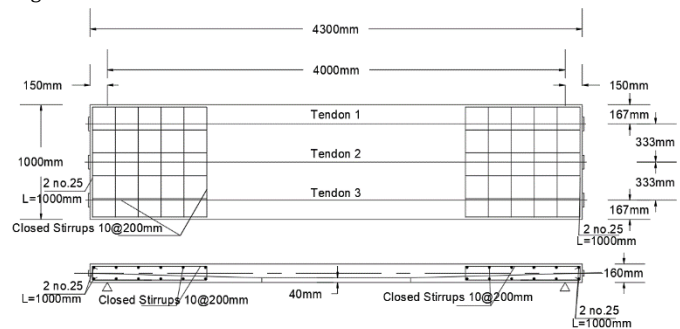
Fig. 3 Post-Tensioned Unbonded Slab cross-section and plan with all reinforcement and tendon detailing (All dimensions are in millimeters)
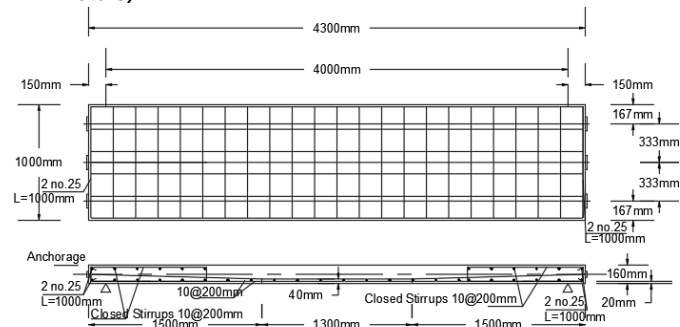
Fig. 4 Post-Tensioned Unbonded Slab cross-section and plan with non-prestressing reinforcement with all the reinforcement and tendons detailing (All dimensions are in millimeters)

3.2 Specimen construction

All specimens were constructed in the AUC structural laboratory; STRANDS performed all prestressing operations. Figure 5 shows the four specimens' formwork and steel reinforcement detailing before and after casting. Six standard cubes of concrete were prepared and tested in 7 days and on the day of testing the specimens under four-point loading flexural test. The average compressive strength at 7-days is 26.4 MPa, while the compressive strength at 28-days is 40 MPa.

(a)

(b)

Fig. 5 (a) The six one-way post-tensioned slab specimens before concrete casting

(b) Post-tensioned Slab specimens after concrete casting

The four specimens are prestressed at the age of 7 days from one live end using a hydraulic jack, to a maximum force of 150 kN. Tendons were inspected after prestressing to check for slippage that might take places at the dead and the live ends; no slippage was found. A detailed demonstration for the calculations and construction phase is mentioned in a previous publishing (Abdelhalim and Sayed-Ahmed, 2021)

3.3 Test setup

HEB-300 beams are used to build the four-point loading test setup for the four simply supported post-tensioned slab specimens. One HEB-300 of length 1.6 meters transfers the load from the loading ram to another two HEB-300 of length 1.0 meters, as shown in Figure 6. The two HEB-300 models exerted the two line- loads exerted on the slab specimens. Rubber pads are placed between the two loading beams and the specimen to avoid any stress concentration. Slabs are supported on steel rollers located with an edge distance of 0.15m.

Fig. 6 The full setup of one of the specimens showing the rubber pads located between the loading beams and the specimen

Ten-millimeter strain gauges were attached to one steel wire of each tendon in each specimen to measure the tendon's strain. However, some of the strain gauges were detached during the casting and pre-tensioning stages. To overcome this issue, 4 LVDTs were used to measure the deflection of UBRS1 at the midpoint, loading beam locations and on one side halfway between the loading beam and the support. Five linear variable differential transducers (LVDTs) were used to measure the deflection of one side of UBS1, UBS2 and UBRS2 at the midpoint and at distances of 40, 90, 130 and 170 cm from the center. Slabs were assumed and further confirmed from the readings of UBRS1 to deform symmetrically and thus the deflection profiles were plotted. The deflection profiles were then used to back calculate the strains in tendons using the first principles. Figure 7 shows the locations of 5 LVDTs along the centerline of the slab.

Fig. 7 UBSR1 specimen with the LVDTs fixed in their positions

UBSR1 was first tested under four-point loading test using displacement control mode of 4 mm/min until the actuator reached its maximum stroke without causing considerable damage to the specimen. Shim plates were added to account for the plastic deformation then the test was restarted using load control mode. The rest of the tests were conducted using load control mode and actuator did not reach its maximum stroke since the other specimens were less ductile compared to UBSR1.

4. Experimental Results

Table 1 shows the maximum deflection, the failure loads and the total loads considering the self-weight of the loading beams for the four tested specimens. Also, the recorded average tendon's strain values at mid-span at failure are mentioned for the four slab specimens.

Table 1. The four slab specimens recorded results

Specimen	Maximum deflection at failure (mm)	Average tendon strain at failure	Failure Load	Total Failure Load
UBS1	87.0	0.009933	58	61.8
UBS2	91.6	0.010833	61	64.8
UBSR1	98.1	0.01076	100	103.8
UBSR2	93.60	0.010605	97.8	101.6

4.1 Unbonded slab series (UBS1 & UBS2)

In both UBS1 and UBS2, the tendons first yielded initiating tension cracks at the bottom. These cracks propagated upward followed by concrete crushing at the top. Failure loads and deflections for UBS1 and UBS2 are 61.8 kN and 64.8 kN as shown in Table 1.

Some differences in crack pattern were observed between UBS1 and UBS2. In specimen UBS1, only one wide crack formed at the onset of failure (under the loading beam). Specimen UBS2 featured this same wide crack in addition to another fine crack at mid span, on the bottom concrete surface (i.e., the tension surface). Both UBS1 and UBS2 rebounded upon unloading by almost 80%; the crack almost closed again. Figure 8 shows the load-deformation curves for both specimens, while Figure 9 shows UBS2 after failure and unloading.

Both specimens' profiles were drawn to calculate the change in length that took place after the application of the load till failure. Table 2 shows the prestressing strain, strain at failure and the total strain of each tendon of UBS1 and UBS2 at mid-span. Again, all tendons in both specimens have surpassed the yielding strain.

Table 2. Strain at failure in each tendon for the four specimens

Specimen	Tendon number	Prestressing Strain	Strain at Failure	Total Strain
UBS1	Tendon 1	0.007551	0.002	0.00955
	Tendon 2	0.007899	0.002	0.00989
	Tendon 3	0.008364	0.002	0.01036
UBS2	Tendon 1	0.007899	0.002976	0.0109
	Tendon 2	0.007551	0.002976	0.0105
	Tendon 3	0.008132	0.002976	0.0111
UBSR1	Tendon 1	0.007783	0.002976	0.01076
	Tendon 2	0.007667	0.002976	0.01064
	Tendon 3	0.007899	0.002976	0.01088
UBSR2	Tendon 1	0.007667	0.0032	0.010867
	Tendon 2	0.007203	0.0032	0.010403
	Tendon 3	0.007345	0.0032	0.010545

4.2 Unbonded slab series with crack control reinforcement (UBSR1 & UBSR2)

Both UBSR1 and UBSR2 failed due to the tendon's yielding followed by concrete crushing. The maximum load, displacement, and average tendon strain values at mid-span are shown in Table 1. In both specimens, the tendons exceeded yield at the ultimate state.
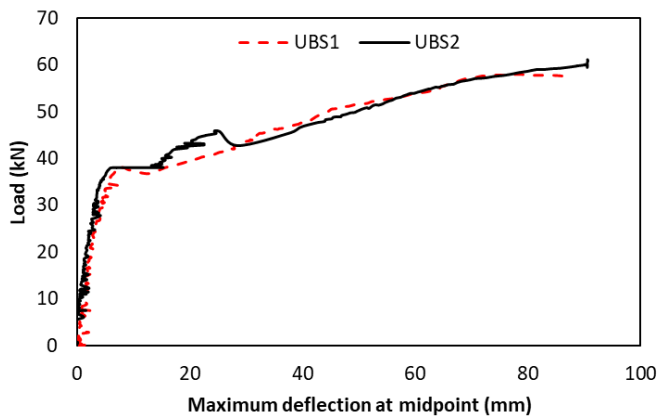
Fig. 8 Load-Deflection curve for data collected from the LVDT located at mid-span for UBS1 and UBS2

Fig. 9 UBS2 after failure and unloading

The observed crack pattern was completely different in this series compared to the UBS series. Instead of a single large crack forming underneath one of the loading beams, fine cracks were distributed all over the bottom surface of both UBSR specimens, as shown in Figure 10. Upon failure, a large crack would form. The large crack forming at failure in specimen UBSR1 was observed to be at mid span, as shown in Figure 11, while in specimen UBSR2 the large crack again formed underneath one of the loading beams, as shown in Figure 12.

Upon unloading after failure, both UBSR1 and UBSR2 rebounded by almost 55%, as shown in Figure 13. The deflected shape of the two specimens is plotted from the obtained LVDT data and the total strain at mid-span calculated in each tendon in specimens UBSR1 and UBSR2 are presented in table 2.

Fig. 10 Cracks formed at UBSR2's bottom surface

Fig. 11 UBSR1 after failure at mid-span

Fig. 12 UBSR2 after failure at the location of the loading beam
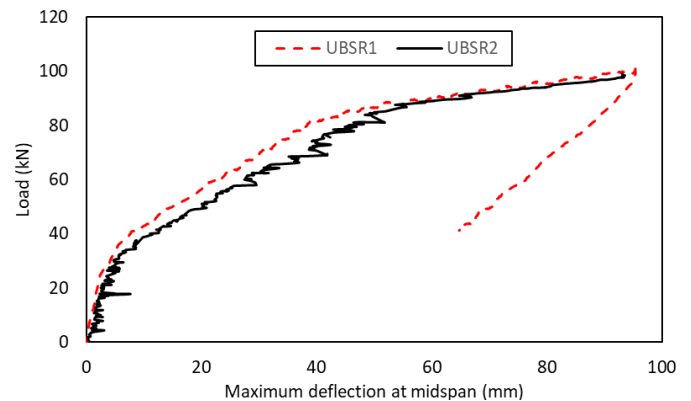
Fig. 13 Load-Deflection curve for data collected from the LVDT located at mid-span for UBSR1 and UBSR2

5. Discussion

Comparing experimental tendon stresses and failure loads to ACI 318-19 provisions

The failure loads for the four post-tensioned slabs were calculated in accordance with ACI 318-19 provisions. Each specimen's jacking force was calculated from the strain measured during the prestressing operation. Short-term losses (elastic shortening, friction and anchorage slippage) were then evaluated. Anchor slippage was neglected as the tendons were checked daily and no slippage was observed. Short-term losses for the four specimens were about 1.7%. Long-term losses (caused by concrete creep, relaxation of steel, and shrinkage) were calculated to an approximate value of 7.7%. Using these quantities, the initial and effective prestressing forces were calculated for each specimen. Initial prestressing force is the force after short-term losses while the effective prestressing force is the force after the deduction of the long-term losses. The consequent tensile and compressive stresses are checked against the ACI 318-19 transfer and service stress limits, sections 24.5.2.1, 24.5.3.1, 24.5.3.2 and 24.5.4.1; the four specimens satisfied all relevant stress limits. The failure load of the unbonded system was calculated using the empirical provisions of 20.3.2.4.1, ACI 318-19.

The ACI 318-19's failure loads and tendon stresses are compared to the experimental data in Figure 14. As expected, the strength of unbonded slabs with crack control reinforcement were predicted by ACI 318-19 to be higher than these with no non-prestressed reinforcement owing to the contribution of the crack control reinforcement to the flexural capacity.
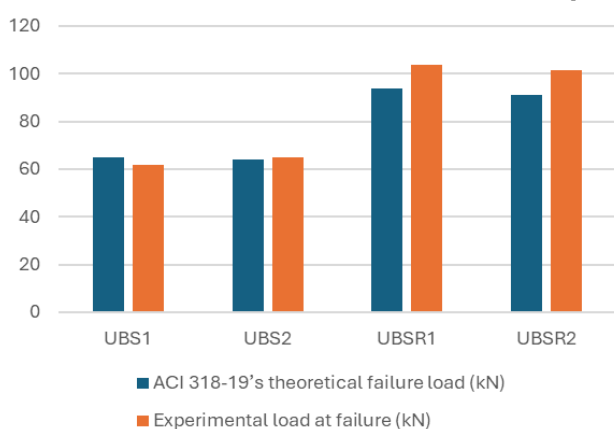
Figure 14 Experimental and analytical failure and tendons stresses

The UBS specimens reached an ultimate experimental load almost equal to that predicted by the ACI 318-19 empirical equation; the difference between the code and experimental failure loads for UBS1 and UBS2 is less than 1%. While the experimental failure loads obtained for the UBSR series slabs are higher than the code-predicted values by almost 10%. Despite the observed accuracy, the limitations governed by the ACI 318-19 on the unbonded tendon's ultimate stress are clearly ill-founded as all the tendons in the two unbonded systems have surpassed the yielding limit.

Influence of crack control reinforcement

The ductility of the two sets is assessed through the maximum deflection achieved by the slabs at mid-span location. The unbonded slabs with non-prestressing reinforcement (UBSR1 and UBSR2) reached a higher deflection with an average of 95.8mm, while the unbonded slabs with no non-prestressed reinforcement (UBS1 and UBS2) reached a smaller deflection with an average of 89.3mm. The unbonded system with non-prestressing steel reinforcement is more ductile than the unbonded system with no non-prestressing.

Also, the addition of non-prestressed steel reinforcement increased the capacity of the unbonded slabs by almost 60%. The addition of the non-prestressing steel reinforcement distributed the cracks and made them finer in width.

After specimens were deemed to fail, the load was gradually removed, and the slabs showed significant rebound. UBS1 and UBS2 slabs have rebounded back by almost 80% in which the cracks generated had almost closed again while UBSR1 and UBSR2 slabs have rebounded back by almost 55%. The difference between the rebound values of the two sets of unbonded slabs is due to the deformation of the crack control reinforcement that limits the rebound of UBSR1 and UBSR2.

6. Conclusion

The adequacy of ACI 318-19 design procedures for unbonded post-tensioned flexural members was investigated, as current provisions are punitive enough to discourage the use of unbonded post-tensioned construction even in situations where it is inherently advantageous. Specifically, the limitations on tendon ultimate stress are overly conservative, and the stipulation that minimum crack control reinforcement be included in unbonded members is not applied to bonded members. Previous research agrees that ACI 318-19's empirical ultimate tendon stress limits for unbonded specimens are conservative. Four simply supported slabs with variable post-tensioning techniques and inclusion of crack control reinforcement were tested to investigate the adequacy of both of ACI 318-19's ultimate tendon stress and minimum crack control reinforcement provisions for unbonded post-tensioning specimens. These slabs were tested in four-point bending to failure; experimentally obtained failure loads, deflections, tendon stresses, crack patterns, and rebounds were compared amongst each other as well as to ACI 318-19 predicted values where appropriate. Critical analysis of the results yielded the following conclusions:

- The addition of crack control non-prestressed steel increased the flexural capacity of the slabs by 60%, reduced the maximum crack width and increased slabs ductility.
- The unbonded slabs with no non-prestressing steel reinforcement have the highest rebound capacity followed by the unbonded slabs with non-prestressing reinforcement.
- Failure loads predicted by ACI 318-19 were reasonably accurate in all tested cases. However, ACI 318-19 predicted that tendons would not yield in all unbonded specimens, contrary to experimental results.

References

Aalami, B. (1994). Unbonded and Bonded Post-Tensioning Systems in Building Construction: A Design and Performance Review. PTI Technical Notes, 5th ser.

Abdelhalim, J. O., & Sayed-Ahmed, E. Y., (2021). Post Tensioned Slab's Testing Program and Setup. International Journal of Civil Infrastructure, 4, 138-143. https://Doi: 10.11159/ijci.2021.017

ACI Committee 318. (2019) Building Code Requirements for Structural Concrete (ACI 318–2019) and Commentary (ACI 318–2019). American Concrete Institute.

Bondy, K. (2012). Two-Way Post-Tension Slabs with Bonded Tendons. PTI Journal.

Bondy, B.K., Gupta, P.R., Alkhairi, F., & Neff, T.L. (2006) Post-tensioning Manual (sixth edition). Phoenix, AZ.

Cooke, N., Park, R., & Yong, P. (1981). Flexural Strength of Prestressed Concrete Members with Unbonded Tendons. PCI Journal, 26, 52-81. https://doi:10.15554/pcij.11011981.52.81

Ellobody, E., & Bailey, C. (2008). Behavior of Unbonded Post-Tension One-way Concrete Slabs. Advances in Structural Engineering, 11(1), 107-120. https://doi:10.1260/136943308784069504

Harajli, M. (2006). On The Stress in Unbonded Tendons at Ultimate: Critical Assessment and Proposed Changes. ACI Structural Journal, 103, 803-812.

He, Z., & Liu, Z. (2010). Stresses in External and Internal Unbonded Tendons: Unified Methodology and Design Equations. Journal of Structural Engineering, 136(9), 1055-1065. https://doi:10.1061/(asce)st.1943-541x.0000202

Hussien, O. et al. (2012) Behavior of bonded and unbonded prestressed normal and high strength concrete beams, HBRC Journal, Volume 8, Issue 3, 2012, Pages 239-251, ISSN 1687-4048. https://doi.org/10.1016/j.hbrcj.2012.10.008.

Kang, T. H., Huang, Y., Shin, M., Lee, J. D., & Cho, A. S. (2015). Experimental and Numerical Assessment of Bonded and Unbonded Post-Tension Concrete Members. ACI Structural Journal, 112(6). https://doi:10.14359/51688194

Mattock, A. H., Yamazaki, J., & Kattula, B. T. (1971). Comparative Study of Prestressed Concrete Beams, with and without Bond. ACI Journal Proceedings, 68(2), 116-125. https://doi:10.14359/11298

Mojtahedi, S., & Gamble, W. L. (1978). Ultimate Steel Stresses in Unbonded Prestressed Concrete. Journal of the Structural Division ASCE, 1159-1165.

Naaman, A. E., & Alkairi, F. (1991). Stress at Ultimate in Unbonded Post-Tensioning Tendons: PART 1-Evaluationof the State-of-the-Art. ACI Structural Journal, 88(5). https://doi:10.14359/2763

Oukaili, N. & Peera, I. (2022) Behavioral nonlinear modeling of prestressed concrete flexural members with internally unbonded steel strands, Results in Engineering, Volume 14, 2022, ISSN 2590-1230, https://doi.org/10.1016/j.rineng.2022.100411.

Süleymanoğlu, H., Uzel, A., & Arslan, G. (2017). Use of Post-Tension Concrete Slabs for Sustainable Design of Buildings. High Tech Concrete: Where Technology and Engineering Meet, 2390-2395. https://doi:10.1007/978-3-319-59471-2_272

Yang, K., Mun, J., & Kim, G. (2013). Flexural Behavior of Post-Tension Normal-Strength Lightweight Concrete One-way Slabs. Engineering Structures, 56, 1295-1307. https://doi: 10.1016/j.engstruct.2013.07.004